Available online at www.sciencedirect.com
ScienceDirect
Journal of the European Ceramic Society 28 (2008) 585–590
www.elsevier.com/locate/jeurceramsoc

Structure and microwave dielectric characteristics of $Ca_{1-x}Nd_{2x/3}TiO_3$ ceramics

M.S. Fu, X.Q. Liu, X.M. Chen *

Department of Materials Science and Engineering, Zhejiang University, Hangzhou 310027, China

Received 14 February 2007; received in revised form 23 May 2007; accepted 9 June 2007
Available online 8 November 2007

Abstract

Dense $Ca_{1-x}Nd_{2x/3}TiO_3$ ceramics with $x = 0.30$, 0.39 and 0.48 were prepared by a solid-state reaction process, and the crystal structure was determined together with the microwave dielectric characterization. The tilted orthorhombic perovskite structure in space group *Pnma* was refined in the present ceramics where a minor amount of TiO_2 was detected as the secondary phase. The microwave dielectric characteristics were strongly affected by the Nd^{3+} concentration and the processing conditions. The best combination of microwave dielectric characteristics was obtained for the as-sintered samples with $x = 0.39$: $\varepsilon_r = 103$, Qf = 15340 GHz and $\tau_f = 247$ ppm/°C. Especially, a sharp decrease of Qf was observed for samples with $x = 0.39$ after annealing in oxygen. Both the dielectric constant and temperature coefficient of resonant frequency of the present ceramics were dependent on the bond valence of the octahedral site. Dielectric loss was significantly affected by the lattice defects and the disordered charge distribution.

Keywords: $CaTiO_3$; Microwave dielectrics; Dielectric loss; Crystal structure

1. Introduction

The perovskite paraelectric titanates, such as $CaTiO_3$ and $SrTiO_3$, have attracted much attention as microwave dielectric materials because of their high dielectric constant[1]. However, their dielectric loss is rather high compared with the complex perovskites. So far, much work has been performed to control the microwave dielectric loss in the perovskite titanates especially those through A- and/or B-site substitution within the ABO_3 structure. Mechanism of B-site substitution was even widely investigated and the factors affecting the microwave dielectric properties were commonly accepted such as cation ordering on B-site[2,3], ordering induced domain boundaries[4] and tilting of oxygen octahedra[5], etc. Monovalent alkali metals and trivalent lanthanide atoms co-substitution with the A-site divalent atoms has been reported by Takahashi et al.[5], and they found that the microwave dielectric characteristics varied with different substitution, but the obvious improvement in the combination of microwave dielectric characteristics could not be obtained.

Recently, substitution of Ca^{2+} by lanthanide (trivalent ions as La^{3+}, Sm^{3+} and Nd^{3+}) ion in $CaTiO_3$ has been investigated by several groups[6–8]. In all these systems, high dielectric constants around 100 have been obtained and the negative shifting of temperature coefficients of resonant frequency compared with $CaTiO_3$ has been found. Although the dielectric loss decreased by introducing the trivalent ions on A-sites, it showed different trends for different substitutions. In both the $Ca_{1-x}La_{2x/3}O_3$[6] and $Ca_{1-x}Sm_{2x/3}O_3$[7] system, the Qf value increased with increasing x directly to their solid solubility. But in the $Ca_{1-x}Nd_{2x/3}O_3$ system, the Qf value reached the highest value at $x = 0.39$ in its solid-solution range (up to $x = 0.93$)[8]. Although good microwave dielectric properties were obtained, the effects of trivalent ion substitution on the dielectric characteristics, especially the dielectric loss of $Ca_{1-x}Ln_{2x/3}O_3$ (Ln: La^{3+}, Sm^{3+} and Nd^{3+}) ceramics was not clearly understood yet. Therefore, it should be an important issue to further understand the property–structure relationship and the physical nature.

In the present work, $Ca_{1-x}Nd_{2x/3}O_3$ ceramics with $x = 0.3$, 0.39 and 0.48 are prepared, and the microwave dielectric characteristics are investigated as the functions of composition and processing conditions together with the crystal structure. The factors such as octahedral tilting, bond valence of the octahedral

* Corresponding author.
E-mail address: xmchen@cmsce.zju.edu.cn (X.M. Chen).

0955-2219/$ – see front matter © 2007 Published by Elsevier Ltd.
doi:10.1016/j.jeurceramsoc.2007.06.015

site, point defects and their distribution, etc. are emphasized in discussing the microwave dielectric characteristics.

2. Experimental procedures

$Ca_{1-x}Nd_{2x/3}TiO_3$ ($x = 0.3, 0.39, 0.48$) powder were prepared by a solid-state reaction process where reagent-grade $CaCO_3$ (99.99%), Nd_2O_3 (99.9%) and TiO_2 (99.5%) powders were adopted as the raw materials. The weighed raw materials were mixed by ball milling with zirconia media in distilled water for 24 h, and the mixtures were heated at 1100 °C in air for 3 h after drying. The calcined powders with 6 wt% of PVA, were pressed into disks measuring 12 mm in diameter and 2–6 mm high under a pressure about 98 MPa, and then sintered at 1350 °C in air for 3 h, the heating rate was 5 °C/min. After cooling from the sintering temperature to 1100 °C at a rate of 2 °C/min, the ceramics were cooled inside the furnace naturally. Some of the samples for microwave characterization were annealed at 1150 °C in oxygen and nitrogen for 6 h.The bulk density of specimens with regular shape was calculated by Archimedes method. The crystal phases of sintered samples after crushing and grinding were determined by powder X-ray diffraction (XRD, RIGAKU D/max 2550 PC, Rigaku Co., Tokyo, Japan) analysis, using Cu Kα radiation. The XRD data for Rietveld analysis were collected over the range of $2\theta = 15°$–$130°$ with a step size of 0.02° and a count time of 2 s. The Rietveld refinement was performed using the FULLPROF program[9], and a pseudo-Voigt profile function with preferred orientation was used. And the microstructure observation was performed by scanning electron microscopy (SEM) (JEOL-JSM-5610LV). The microwave dielectric constant ε_r and quality factor Q were evaluated using Hakki–Coleman method and cavity method using vector network analysis (Agilent 87953ES, USA), respectively[10]. Because Q factor generally varies inversely with the frequency, in the microwave region, the product of Qf was used to evaluate the dielectric loss instead of Q. The temperature coefficient of resonant frequency τ_f at microwave frequency was measured in the temperature range from 20 to 85 °C. The measurement error of dielectric constant, temperature coefficient of resonant frequency and Qf value were less than $0.5\% \times \varepsilon_r$, 2 ppm/°C and $1.5\% \times$ Qf, respectively. And the measurement of microwave dielectric properties was carried on several samples for many times.

3. Results and discussion

As shown in Fig. 1, the XRD patterns for the $Ca_{1-x}Nd_{2x/3}TiO_3$ ($x = 0.3, 0.39, 0.48$) ceramics indicate the perovskite major phase combined with just a minor amount of TiO_2 secondary phase. Fig. 2 illustrates the profile fit and difference for the sample with $x = 0.3$, and the orthorhombic major phase in space group *Pnma* is refined together with a minor amount of tetragonal TiO_2 in space group *P*42/*mnm*. Experimental parameters for X-ray powder diffraction of $Ca_{1-x}Nd_{2x/3}TiO_3$ ceramics and the TiO_2 second phase are shown in Table 1. The smaller size of Nd^{3+} ion (1.27 Å) than Ca^{2+} ion (1.34 Å) and the A-site vacancies cause the tolerance factor (t) of the ceramics decreases from

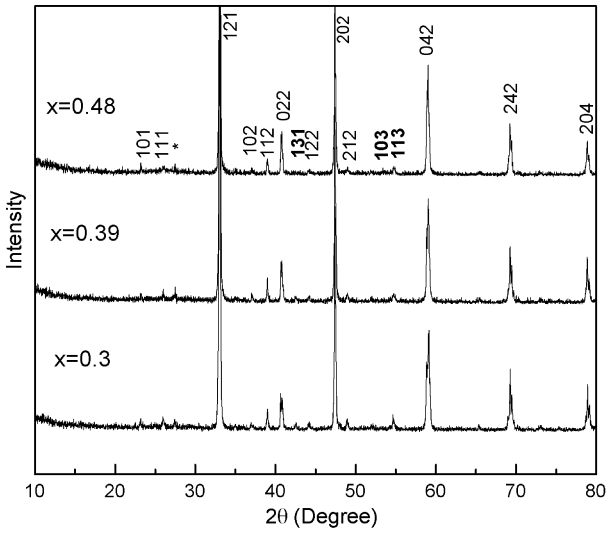

Fig. 1. XRD patterns of $Ca_{1-x}Nd_{2x/3}TiO_3$ ceramics sintered at 1350 °C for 3 h, indicating an orthorhombic major phase combined with a micro amount of TiO_2 (*).

0.914 to 0.856 with increasing x. As reported by Reaney et al.,[11] the tilting of oxygen octahedra occurs in both anti-phase and in-phase when $t < 0.965$. So, superlattice reflections (marked in bold) which indicate that oxygen octahedra around Ti^{4+} tilted in the $Ca_{1-x}Nd_{2x/3}TiO_3$ system are detected in the XRD patterns,. According to Glazer's theory[12], the reflections of odd-odd-odd with $k \neq 1$ are assigned to an anti-phase tilting along pseudocubic [1 0 0] direction (denoted by a^-) of the oxygen octahedra and the odd-even-odd reflections with $h \neq 1$ are assigned to an in-phase tilting along pseudocubic [0 1 0] direction (denoted by b^+). So the (1 3 1), (1 1 3) reflections indicate an a^- tilting and the (1 0 3) reflection indicate $a\,b^+$ tilting. The tilting mechanism defined by the present combination of the distortions is consistent with the orthorhombic $a^-a^-b^+$ tilt system with space group *Pnma* according to Glazer's notation[13]. Fig. 3 gives the

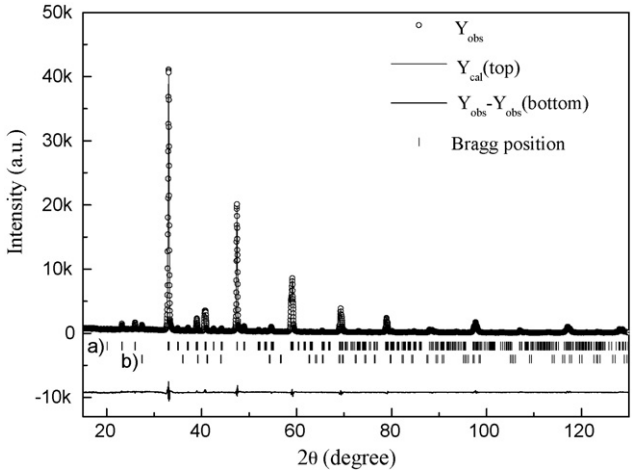

Fig. 2. X-ray powder diffraction patterns obtained at room temperature (circles) and calculated (solid line) of $Ca_{1-x}Nd_{2x/3}TiO_3$ ceramics with $x = 0.3$. Vertical marks show the position of allowed structural Bragg reflections for (a) $Ca_{1-x}Nd_{2x/3}TiO_3$ and (b) TiO2. A difference curve is plotted at the bottom of the pattern.

Table 1
Experimental parameters for X-ray powder diffraction of $Ca_{1-x}Nd_{2x/3}TiO_3$ ceramics

		$x=0.30$	$x=0.39$	$x=0.48$
The main phase	Unit cell (space group *Pnma*, 62)	$a=5.4397(1)$ Å $b=7.6628(2)$ Å $c=5.4026(1)$ Å $V=225.201(9)$ Å^3	$a=5.4387(2)$ Å $b=7.6671(2)$ Å $c=5.4084(2)$ Å $V=225.53(1)$ Å^3	$a=5.4370(2)$ Å $b=7.6710(2)$ Å $c=5.4102(2)$ Å $V=225.645(1)$Å^3
	Fraction (wt%)	96.9(5)	97.3(5)	94.0(6)
The second phase (TiO_2)	Unit cell (space group *P*42/*mnm*, 136)	$a=4.5986(5)$ Å $b=4.5986(5)$ Å $c=2.9638(9)$ Å $V=62.67(9)$ Å^3	$a=4.5953(4)$ Å $b=4.5953(4)$ Å $c=2.9605(8)$ Å $V=62.51(9)$ Å^3	$a=4.5973(0)$ Å $b=4.5973(0)$ Å $c=2.9583(0)$ Å $V=62.52(4)$ Å^3
	Fraction (wt%)	4.0(5)	3.6(5)	5.9(4)
R_p (profile)		5.77	6.14	6.53
R_{wp} (weighted profile)		7.53	7.97	8.92
R_B (Bragg)		3.66	3.66	4.48
R_F		4.26	5.16	4.25
Reduced χ^2		3.00	4.67	4.10
B_{iso} (Å^2) of Nd^{3+}		1.932	1.992	1.923

crystal structure of the $Ca_{1-x}Nd_{2x/3}TiO_3$ ceramics. The conterminal oxygen octahedra tilted in the opposite direction along the pseudocubic [1 0 0] and [0 0 1] axes but in the same direction along the [0 1 0] axis, which illustrated the $a^-a^-b^+$ tilting system visually.

Fig. 4(a) shows the dielectric constant and temperature coefficient of resonant frequency of $Ca_{1-x}Nd_{2x/3}TiO_3$ ceramics as functions of x. Both the dielectric constant ε_r and the temperature coefficient of resonant frequency τ_f of the as-sintered ceramics decrease with increasing x nonlinearly, from 113 to 100 for the former and from 300 to 207 ppm/°C for the latter. $CaTiO_3$ belong to incipient ferroelectric and the high dielectric constant is attributed to the rattling of the small Ti^{4+} cations in the oxygen octahedra[14]. Shannon[15] suggested that the deviation of "observed" polarizability (α_{obs}) from "theoretical" polarizibility (α_{theo}) arises when the cation rattling occurs in the structural sites. Table 2 shows the calculated theoretical and observed polarizibility using summation rule[15] and Claussius–Mossotti relation[16]. The deviation of α_{obs} from α_{theo} decreases together with dielectric constant as x increases, which might be due to the increased compression of rattling of Ti^{4+} cations. The decreasing B–O distances and increasing B-site bond valence shown in Table 2 indicate that the compression of cation rattling increases as x increases.

The temperature coefficient of resonant frequency can be expressed by Eqs. (1) (differentiating the macroscopic

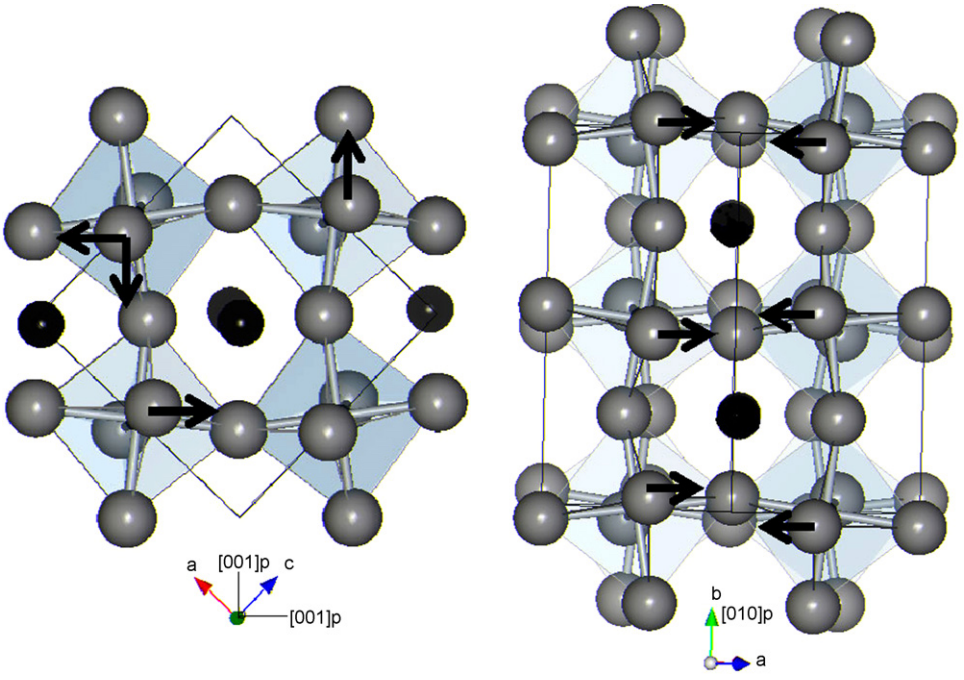

Fig. 3. Crystal structure of $Ca_{1-x}Nd_{2x/3}TiO_3$ ceramic with $x=0.3$ drawn with VENUS[23].

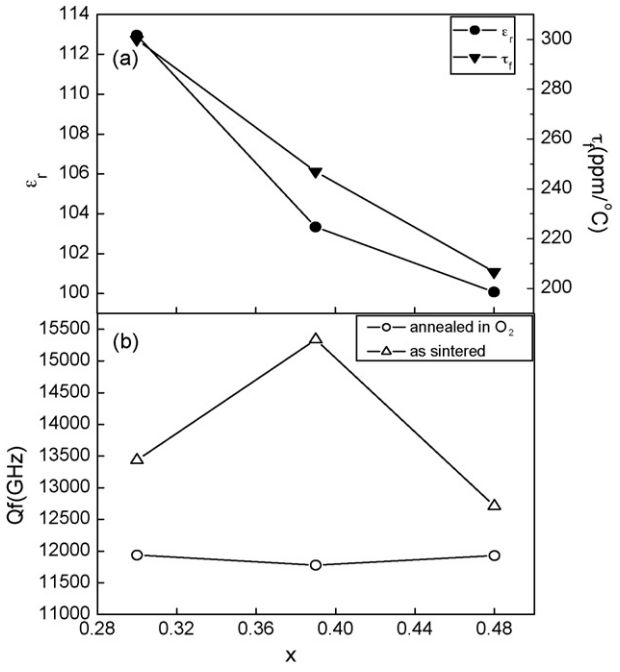

Fig. 4. Microwave dielectric properties of $Ca_{1-x}Nd_{2x/3}TiO_3$ ceramics as functions of x: (a) dielectric constant and temperature coefficient of resonant frequency; (b) Qf value for as-sintered and O_2-annealed samples.

Clausius–Mossotti equation) and (2)[17].

$$\tau\varepsilon_r = \frac{1}{\varepsilon_r}\left(\frac{\partial\varepsilon}{\partial T}\right)_P = \frac{(\varepsilon_r-1)(\varepsilon_r+2)}{\varepsilon_r}(A+B+C) \quad (1)$$

$$A = -\frac{1}{3V}\left(\frac{\partial V}{\partial T}\right)_P, \qquad B = \frac{1}{3\alpha_m}\left(\frac{\partial\alpha_m}{\partial V}\right)_T\left(\frac{\partial V}{\partial T}\right)_P,$$

$$C = \frac{1}{3\alpha_m}\left(\frac{\partial\alpha_m}{\partial T}\right)_V, \qquad \tau_f = -\frac{\tau\varepsilon_r}{2} - \alpha \quad (2)$$

where α is the thermal expansion coefficient. For incipient ferroelectric materials, the large permittivities are often accompanied by the large negative temperature coefficient of relative permittivity. That is because the primary factor affecting $\tau\varepsilon_r$ is $(\partial\alpha_m/\partial T)_V$ which is always negative for materials with $\varepsilon_r > 10$, and decreases with increasing permittivity in the range $10 < \varepsilon_r < 200$[17]. As the contribution from $(\partial\alpha_m/\partial T)_V$ increases, $\tau\varepsilon_r$ becomes more negative and the magnitude of the change is amplified by larger ε_r values. So the $Ca_{1-x}Nd_{2x/3}TiO_3$ ceramics have large positive τ_f values. On the other hand, the increased values of $(\partial\alpha_m/\partial T)_V$ accompanied with the decreased ε_r in the present ceramics might be the major reason for the decreased τ_f as x increases. As reported by Collar et al.,[18] another factor, the octahedra tilting, will affect τ_f. τ_f moves towards negative as the tilting increases. In the present system, the decreased tolerance factor and increased B-site valence indicate that the tilting enhances with increasing x, and this is another reason for the decreasing τ_f.

Fig. 4(b) shows the variation of Qf value of $Ca_{1-x}Nd_{2x/3}TiO_3$ ceramics sintered under different conditions. The Qf value of the as-sintered sample with $x = 0.39$ (Qf = 15340 GHz) is much higher than those for the neighbor compositions (13440 GHz for $x = 0.3$ and 12710 GHz for $x = 0.48$). The similar results have been reported by Yoshida et al.[8], but why the abnormality of Qf value at $x = 0.39$ existed had not been mentioned. Kim et al.[6] suggested that the increased Qf value in the $Ca_{1-x}La_{2x/3}O_3$ system was due to the ordered arrangement of the cations and the vacancies in A-sites, but no ordering superstructure reflection is detected in the XRD patterns with $Ca_{1-x}Nd_{2x/3}TiO_3$ ceramics as shown in Fig. 1. In the $Ca_{1-x}Sm_{2x/3}O_3$ system, Yoon and co-workers[7] suggested that the increased Qf value up to the solid-solution limit ($x = 0.6$) was related to the increased A-site vacancy concentration with increased Sm^{3+} substitution, which might have reduced the anharmonic-interaction-affect dielectric loss[19]. However, the highest Qf value of $Ca_{1-x}Nd_{2x/3}TiO_3$ ceramics exist at $x = 0.39$ far away from the solid-solution limit with $x = 0.93$, which should not be caused by the reducing anharmonic phonon decay processes. The effect of density on Qf values of the present ceramics should also be neglected, because the relative density of this system is above 96% for all the three compositions. Fig. 5 shows the SEM micrographs of $Ca_{1-x}Nd_{2x/3}TiO_3$ ceramics sintered at 1350 °C. The grain size varies from about 5 to 30 μm, but no obvious difference exists among the three compositions. The grain size effects might also have little influence on the dielectric loss. Although the amount of TiO_2 second phase in the sample with $x = 0.39$ is a little smaller than that in other compositions (as shown in Table 1), it would not be the main factor affecting the dielectric loss either. Because the concentration of second phase in the annealed samples (in oxygen) is less than 3% for all compositions, while the Qf values of the annealed samples are lower than the sintered samples for all the compositions as shown in Fig. 4(b). It is also contradictory to our common sense that the Qf values of the annealed samples (in oxygen) decreases to the same level for all compositions here. As generally observed in many titanate ceramics, Ti^{4+} reduction and oxygen vacancy formation always exist during processing and lead to high dielectric loss[20,21]. So the dielectric loss mechanism in the present system should due to the structure and lattice defects. Schlömann[22] pointed out that among many kinds of the

Table 2
Observed and theoretical polarizabilities, B-site bond valences and bond strengths between B-site cation and oxygen in $Ca_{1-x}Nd_{2x/3}TiO_3$ ceramics

Composition	α_{theo} (Å^3)	Observed ($Z = 4$)					Δ (%)
		K	$V_{unit\ cell}$ (Å^3)	α_{obs} (Å^3)	d (B–O) (Å)	V_B	
$x = 0.30$	12.1610	112.96	225.202	13.1074	1.951	4.157	7.22
$x = 0.39$	12.1763	103.35	225.531	13.0770	1.949	4.181	6.89
$x = 0.48$	12.1916	100.08	225.645	13.0714	1.948	4.215	6.73

$\Delta\ (\%) = ((\alpha_{obs} - \alpha_{theo})/\alpha_{obs}) \times 100$.

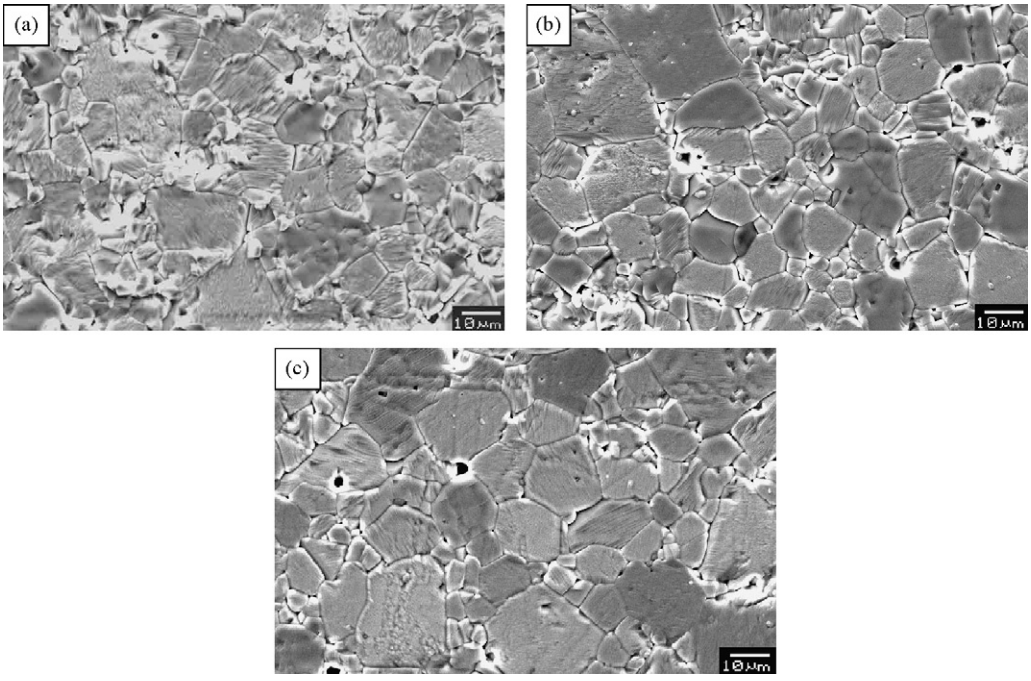

Fig. 5. SEM micrographs of $Ca_{1-x}Nd_{2x/3}TiO_3$ ceramics sintered at 1350 °C for 3 h: (a) $x = 0.3$, (b) $x = 0.39$, and (c) $x = 0.48$.

structure and lattice defects, the disordered charge distribution in crystal has the primary contribution to dielectric loss, and he derived the following equation:

$$\tan\delta \propto \frac{\omega}{C_t^3}\left\{1 - \frac{1}{(1+(\omega/\omega_0)^2)}\right\} \quad (3)$$

where $C_t(\cong 4000\,\text{m/s})$ is the transverse sound velocity, and ω_0 the characteristic frequency given by $\omega_0 = C_t/l$. l is defined as the "correlation distance", the length necessary to maintain the charge neutrality.

In $Ca_{1-x}Nd_{2x/3}TiO_3$ ceramics, there are two kinds of lattice defects that affect the charge distribution. The first one is originated from the Nd^{3+} substitution for Ca^{2+} in $CaTiO_3$, and the defect reaction is given as the following (Kröger–Vink notation):

$$Nd_{2/3}TiO_3 \rightarrow \tfrac{2}{3}Nd_{Ca}^{\bullet} + \tfrac{1}{3}V''_{Ca} + Ti_{Ti}^{x} + 3O_O^x \quad (4)$$

The second one is the familiar oxygen vacancy formation reaction given by:

$$2Ti_{Ti}^{x} + O_O^x \rightarrow 2Ti'_{Ti} + V_O^{\bullet\bullet} + \tfrac{1}{2}O_2 \uparrow \quad (5)$$

The oxygen vacancy formation in titanate ceramics could make charge shift for Ti^{4+} ion to Ti^{3+} and cause the charge distribution disorderly which would increase the dielectric loss. The A-site cation vacancy in the $Ca_{1-x}Nd_{2x/3}TiO_3$ ceramics could react with the oxygen vacancy to reduce the number of oxygen vacancies and maintain the charge neutrality within a small correlation distance:

$$V''_{Ca} + V_O^{\bullet\bullet} \Leftrightarrow 0 \quad (6)$$

However, excess cation vacancy might also cause the disordered charge distribution and the increased correlation distance to maintain the charge neutrality. Therefore, although the annealing process in the present system reduces the concentration of oxygen vacancy, it will increase the correlation distance and subsequently increase the dielectric loss. Low dielectric loss might be obtained when the cation and oxygen vacancies got an appropriate relative concentration to make the correlation distance even small. It might come to an appropriate concentration of both vacancies in the as-sintered samples with $x = 0.39$. As shown in Table 1, the larger Debye–Waller factor of A-site cations at $x = 0.39$ ($B_{iso} = 1.992\,\text{Å}^2$) than neighbor compositions ($1.932\,\text{Å}^2$ for $x = 0.3$ and $1.923\,\text{Å}^2$ for $x = 0.48$) indicates that the Nd^{3+} cation at $x = 0.39$ tends to move away from its equilibrium position more easily to make a short correlation distance. We also prepared some samples annealed in nitrogen to introduce excess oxygen vacancies and the resonant peak could not be detected when the microwave dielectric property measurement was carried on. That is attributed to the high dielectric loss caused by the excess oxygen vacancies, which increased the correlation distance largely. When put the samples to anneal in oxygen again, the Qf values showed the same tendency as shown in Fig. 4(b). These results could also suggest that the oxygen vacancy plays a dominant role in affecting the dielectric loss together with A-site cation vacancy. However, because the containing neodymium causes a color with deep purple of ceramics, no obvious color change correlating to the concentration variation of oxygen vacancies is detected during the annealing processes.

4. Conclusions

Effects of Nd^{3+} concentration and processing conditions upon the microwave dielectric characteristics of $Ca_{1-x}Nd_{2x/3}TiO_3$ ceramics were investigated together with their structure. The tilted orthorhombic perovskite structure in space

group *Pnma* was refined in the present ceramics where a minor amount of TiO_2 was detected as the secondary phase. Both the dielectric constant and temperature coefficient of resonant frequency of the present ceramics decreased with increasing x nonlinearly while the Qf value got the highest value in the as-sintered samples with $x = 0.39$, while the post densification annealing in oxygen caused a sharp decrease in Qf value especially for that of $x = 0.39$. The dielectric constant decreased with increasing x because of the suppression of the cation rattling. The increasing values of $(\partial\alpha_m/\partial T)_V$ accompany with decreasing ε_r and enhanced octahedra tilting of the sintered ceramics might be responsible for the decreased τ_f as x increased. Dielectric loss was affected by both the A-site cation vacancy and the oxygen vacancy. It is effective to minimize the disordered charge distribution for reducing the microwave dielectric loss and improving the Qf value in the present ceramics, and this result may have universal meaning in controlling dielectric loss.

Acknowledgements

This work was financially supported by the National Science Foundation of China under grant number 50332030 and Chinese National Key Project for Fundamental Researches under grant number 2002CB613302.

References

1. Kell, R. C., Greenham, A. C. and Olds, G. C. E., High-permittivity temperature-stable ceramic dielectrics with low microwave loss. *J Am Ceram Soc*, 1974, **56**(7), 352–354.
2. Khalam, L. A., Screemoolanathan, H., Ratheesh, R., Mohanan, P. and Sebatian, M. T., Preparation, characterization and microwave dielectric properties of $Ba(B_{1/2}B'_{1/2})O_3$ ceramics. *Mater Sci Eng*, 2004, **B107**, 264–270.
3. Takahashi, T., First-principles investigation of the phase stability for $Ba(B'^{2+}_{1/3}B''^{5+}_{2/3})O_3$ microwave dielectrics with the complex perovskite structure. *Jpn J Appl Phys*, 2000, **39**, 5637–5641.
4. Davies, P. K. and Tong, J., Effect of ordering-induced domain boundaries on low loss $Ba(Zn_{1/3}Nb_{2/3})O_3$-$BaZrO_3$ perovskite microwave dielectrics. *J Am Ceram Soc*, 1997, **80**(7), 1727–1740.
5. Takahashi, H., Baba, Y., Ezaki, K., Okamato, Y., Shibata, K., Kuroki, K. *et al.*, Dielectric characteristic of $(A^{1+}_{1/2}A^{3+}_{1/2})TiO_3$ ceramics at microwave frequencies. *Jpn J Appl Phys*, 1991, **30**(9B), 2339–2342.
6. Kim, I. S., Jung, W. H., Inaguma, Y., Nakamura, T. and Itoh, M., Dielectric properties of a-site deficient perovskite-type lanthanum-calcium-titanium oxide solid solution system. *Mater Res Bull*, 1995, **30**, 307–316.
7. Kim, W. S., Kim, E. S. and Yoon, K. H., Effects of Sm^{3+} substitution on dielectric properties of $Ca_{1-x}Sm_{2x/3}TiO_3$ ceramics at microwave frequencies. *J Am Ceram Soc*, 1999, **82**(8), 2111–2115.
8. Yoshida, M., Hara, N., Takada, T. and Seki, A., Structure and dielectric properties of $(Ca_{1-x}Nd_{2x/3})TiO_3$. *Jpn J Appl Phys*, 1997, **36**, 6818–6823.
9. Rodriguez-Carvajal, J., "Recent developments of the program FULLPROF", in commission on powder diffraction (IUCr). *Newsletter*, 2001, **26**, 12–19.
10. Kajfez, D. and Guillon, P., *Dielectric resonators* (*2nd ed.*). Noble Publishing Corporation, Atlanta, 1998.
11. Reaney, I. M., Collar, E. L. and Setter, N., Dielectric and structure characteristics of Ba- and Sr-based complex perovskites as a function of tolerance factor. *Jpn J Appl Phys*, 1994, **33**(7A), 3984–3990.
12. Glazer, A. M., Simple ways of determining perovskite structures. *Acta Cryst*, 1975, **A31**, 756–762.
13. Glazer, A. M., The classification of tilted octahera in perovskites. *Acta Cryst*, 1972, **B28**, 3384–3392.
14. Kipkoech, E. R., Azough, F. and Freer, R., Microstructure control of microwave dielectric properties in $CaTiO_3$-$La(Mg_{1/2}Ti_{1/2})O_3$ ceramics. *J Appl Phys*, 2005, **97**, 064103.
15. Shannon, D., Dielectric polarizabilities of ions in oxides and fluorides. *J Appl Phys*, 1993, **73**, 348–366.
16. Roberts, S., Polarizabilities of ions in perovskite-type crystals. *Phys Rev*, 1951, **81**(5), 865–868.
17. Bosman, A. J. and Havinga, E. E., Temperature dependence of dielectric constants of cubic ionic compounds. *Phys Rev*, 1963, **129**(4), 1593–1600.
18. Collar, E. L., Reaney, I. M. and Setter, N., Effect of structural changes in complex perovskites on the temperature coefficient of the relative permittivity. *J Appl Phys*, 1993, **74**(5), 3414–3425.
19. Peltzelt, J., Pacesova, S., Fousek, J., Kamba, J., Zelezny, V., Koukal, V. *et al.*, Dielectric spectra of some ceramics for microwave applications in the range of 1010–1014 Hz. *Ferroelectrics*, 1989, **93**, 77–85.
20. Takada, T., Wang, S. F., Yoshikawa, S., Jang, S. J. and Newnham, R. E., Effect of glass additions on BaO–TiO2–WO3 microwave ceramics. *J Am Ceram Soc*, 1994, **77**(7), 1909–1916.
21. Kim, D. W., Ko, K. H., Kwon, D. K. and Hong, K. S., Origin of microwave dielectric loss in $ZnNb_2O_6$-TiO_2. *J Am Ceram Soc*, 2002, **85**(5), 1169–1172.
22. Schlömann, E., Dielectric losses in ionic crystals with disordered charge distributions. *Phys Rev*, 1964, **135**, A413–A419.
23. Izumi, F. and Dilanian, R. A., *Recent Research Developments in Physics, vol. 3, Part II*. Transworld Research Network, Trivandrum, 2002, ISBN 81-7895-046-4, pp. 699–726.